2015-07-01

Composition Based Modaling of Silicone Nano-Composite Strain Gauges

Daniel Alexander Baradoy
Brigham Young University - Provo

Composition Based Modeling of Silicone Nickel Nano-Composite Strain Sensors with Applications in Fetal Monitoring

Daniel Alexander Baradoy

A thesis submitted to the faculty of
Brigham Young University
in partial fulfillment of the requirements for the degree of

Master of Science

Anton E. Bowden, Chair
David T. Fullwood
Steven K. Charles

Department of Mechanical Engineering

Brigham Young University

July 2015

ABSTRACT

Composition Based Modeling of Silicone Nickel Nano-Composite Strain Sensors with Applications in Fetal Monitoring

Daniel Alexander Baradoy
Department of Mechanical Engineering, BYU
Master of Science

In this work a review of the technology surrounding high deflection strain sensing with an emphasis on that of a recently developed nickel nano-composite strain sensor is presented. A new base silicone material was identified for the nickel nano-composite strain sensor that improves its mechanical stiffness and conductive properties. A previously identified cyclic creep concern was mitigated through preconditioning and the use of adhered backing materials.

Through a block design experiment the strain/resistance curves for the strain sensors were characterized over a wide range of nano-filler material compositions. An analytical model was developed based on observation that the resistance of the sensors follows a log-normal response with respect to applied strain. The model demonstrated high fidelity in representing the resistance-strain relationship of the sensors yielding an average R^2 value of .93. A standard least squares statistical analysis confirmed strong relationships between curve fit parameters of the modified log-normal model and additive volume fractions with significance at the .05 level for each case.

A suitable strain gauge composition was selected for a specific application: a fetal monitoring device. A prototype belt was developed that is worn over the abdomen to detect deflections cause by labor contractions and other fetal movements. Simulation testing on the device was performed and the device was found to be a feasible option for fetal monitoring.

Keywords: nano-composite, strain, high deflection, fetal monitoring

ACKNOWLEDGEMENTS

I would like to give a special thanks to all those who assisted me through my research process. Dr. Bowden and Dr. Fullwood who spent many hours mentoring me and reviewing my work, my peers in both the BABEL lab and the Smart Materials lab who motivated and inspired my efforts and my wife who without reservation supported my time consuming endeavors. Thanks and consideration is also given to Dr. Charles for his service on my graduate committee.

This work was made possible in part by the funding provided by the National Science Foundation under the grant number CMMI-1235365. Any opinions, findings, and conclusions or recommendations expressed in this material are those of the author(s) and do not necessarily reflect the views of the National Science Foundation.

TABLE OF CONTENTS

LIST OF TABLES

LIST OF FIGURES

CHAPTER 1. INTRODUCTION

This thesis focuses on the development, improvement and modeling of silicone nano-composite strain gauges with a specific application in the area of fetal monitoring. Much of the science behind the physical phenomena that allows this composite material to be used as a sensor has already been explored, and models have been created which predict gauge behavior based on the interactions of conductive particles at the nano and mirco scale, but no model has been developed working backwards from observed gauge behavior and then relating this behavior to composition. This thesis will describe the research conducted in order to overcome specific, previously identified limitations of the sensors with respect to creep, strain range, and elastic modulus. I also characterize the refined strain gauges and develop a model for the strain/resistance curves of the sensors based on nanofiller composition. Finally, I include specific application of the refined sensors to applications in fetal monitoring.

Chapter 2 includes a background of high deflection strain gauges including mercury in rubber tubes, other nano-composite technologies and an emerging sensor using conductive films on elastomers. A review of the previous work done on silicone nickel nano-composite gauges will be given as to provide a takeoff platform for the current work. Also provided in the thesis is the process of new material selection and the measures taken to mitigate permanent deformation including preconditioning and applying backings.

Chapter 3 is a copy of the journal paper written on the characterization and modeling of the strain gauges through a block design experiment. Resistance curves for a relevant range of

compositions are found and discussed. A model based on a log-normal distribution curve is used to describe the shape of the strain/resistance curves. The parameters used in this curve fit are then correlated to the volume fractions of additives used in each sample gauge. My co-authors on this paper are Anton Bowden and David Fullwood.

Chapter 4 describes a specific application of the piezoresistive strain gauge technology to fetal monitoring. A piezoresistive strain gauge was incorporated into an abdominal belt capable of tracking the deflections of a mother's abdomen due to labor contractions or other fetal movements. Deflection data from the strain gauge was interpreted via an integrated microcomputer and transmitted wirelessly to a nearby computer. Proof-of-concept testing demonstrated viability of the device and recommendations for further testing and development are given.

Chapter 5 summarizes the contributions of my thesis and provides suggestions regarding directions for further follow-on research.

CHAPTER 2. HIGH DEFLECTION STRAIN GAUGE DEVELOPMENT

2.1 Introduction

The advancement of strain gauge technology has seen vast improvements since the invention of the metallic foil gauge in the late 30's [1] . Although the technology has progressed a great deal and is used in systems in ways they were not before, limitations still exist such as mobility and robustness, but most of all, the low degree of strain which they can detect. These limitations of the foil gauge still cause them to be primarily used in laboratory or carefully controlled settings.

Strain gauges can be quantified by two measures: Effective sensing strain and strain sensitivity. Sensitivity is often reported as the gauge factor. Gauge factor is the change in resistance over the nominal resistance divided by the strain. Higher gauge factors indicate a larger resistance change over a smaller strain and thereby a more accurate sensor.

In an effort to overcome these problems, various types of high deflection strain gauges (HDSG) have been developed over the last several decades. Although the apparent function HDSG's seem to operate in a similar fashion to conventional strain gauges, fundamentally different physical principles drive the changes in resistance that are tracked. Metal foil gauges change resistance as a single continuous strip metal is deformed while silicone nano-composite gauges rely entirely on the interactions and spacing between particles that change as strain is applied. The larger degree of strain that these sensors are capable of detecting has permitted them to be integrated into systems where conventional strain gauges would be of no use.

One group of HDSG's that has been studied extensively at BYU is nano-composite elastomeric gauges. Nickel nano-particles are embedded into silicones to produce a conductive composite that changes electrical resistance proportional to strain.

The purpose of this chapter is to describe improvements in material composition for these sensors that has increased the range of detectable strain and reduced the volume of nano-particles needed to be conductive enough for use.. A novel method of tailoring the mechanical response of the sensor separately from its electrical response through the use of an integrated non-conductive backing material is introduced. Various backing materials for the gauges were examined with the goal of improving the longevity and resilience of the sensors.

2.2 Background of HDSG's

A commonly used strain gauge is the metal foil gauge. This sensor uses a patterned strip of thin metal that is adhered onto the surface where the strain is being measured. When it experiences a strain the foil strips are either elongated or compressed, which causes a change in electrical resistance proportional to the strain. The resistance change is recorded and converted into the corresponding strain for analysis. Unfortunately, these sensors are only capable of strains under 5% with gauge factors ranging from 2-5 [1] and are usually limited to use in a laboratory setting.

Due to the limitations of this type of strain gauge there has been much work done exploring other options for strain tracking. Some of these include sensors that are specifically designed to detect large strains exceeding the capabilities of the metal foil gauges.

Optical fiber strain gauges are another type of sensor that are typically very accurate at measuring small strains and have some benefits over the conventional metal foil type. These

sensors do not function on the same principal as the others. Instead of measuring a change in resistance they measure a change in the wavelength of the light that travels along the fibers. They are useable over a large range of temperatures and are not affected by changing temperatures. They can also have massive cable lengths leading to the sensor allowing them to be placed at large distances from the data acquisition site [2,3]. Recently, work has been done to replace the normally used silica fibers with a polymer fiber allowing the sensor to detect larger strains up to 15% [3,4]with an equivalent gauge factor of .8 [5,6].

Another example is the "mercury in a rubber tube" sensor. This works on the same general principle as the conventional gauge in that resistance is tracked and then equated to a strain. As a rubber tube filled with mercury is elongated, the cross sectional area decreases and the length increases, thereby increasing the resistance of the system. This sensor has been used for biomedical purposes such as heart rate, breathing and blood flow monitors [7,8]. Because this gauge is primarily used in the medical field, data on its sensing capabilities from an engineering standpoint is not available.

Other large strain sensors use elastomers with conductive micro or nano-particles embedded in them [9]. Some of the most recent technologies include synthetic rubbers with carbon nanotubes as a conductive additive [10]. These have been used as high deflection strain gauges or compressive pressure sensors [11]. Many have been reported as being able to detect strain up to 100% over thousands of cycles with little variability in readings [12]. Accuracy of these sensors depends upon the composition of the sensor. One study in particular used Carbon Black embedded in polydimethylsiloxane (PDMS) and found deflection capabilities over 200% but only effective strain sensing up to 25% with a gauge factor of 29 [13].

Some of these strain gauges with an elastomer base do not use filler materials, but rather a thin conductive coating bonded onto the surface of the base material. One example is the graphene on rubber gauge with strain detection up to 200% and a gauge factor of 45 [14,15]. A similar technology uses graphene woven fabrics that become more electrically resistive as the fabric experiences tensile loads. These strain gauges have a range of 0-15% with gauge factor of 20 [16].

Table 2.1 summarizes currently available strain gauges along with their approximate range of use and accuracy.

Table 2.1 – Strain ranges and gauge factors for various sensor technologies

Type	Metal Foil	Fiber Optic	Silica Fiber Optic	Carbon Black in PDMS	Graphene on Rubber	Graphene Woven
Effective Range (%)	< 5	< 5	< 15	< 25	< 200	< 15
Gauge Factor	2-5	.8	.8	20-30	45	1000

2.3 Nano-Composite Gauges

Silicone nano-composite strain gauges use a silicone base material with nickel nano-particles embedded in it. 3 types of additives are used: Nickel nanostrands (NiNs), nickel coated carbon fiber (NCCF) and Novamet. NiNs and Novamet have matrix like structures at the nano scale while NCCF are on the micro scale. Changes to the orientations of these particles with respect to each other cause a change in resistance of the bulk material. This makes these strain gauges work in a similar fashion to the existing technology [17]. One interesting difference is that these nano-composite gauges decrease in electrical resistance instead of increase when a strain is applied.

The unique electrical behavior of this material has been described in previous BYU research using a model based on percolation and quantum tunneling between nano-particles as strain is introduced [18]. Each location where nano-particles are separated by a layer of the base silicone material is referred to as a gap. Gap sizes change with strain, which directly affects the probability that quantum tunneling may occur, thereby changing the likelihood of a conductive percolative network being formed across the bulk material. In essence the gaps perform as individual variable resistors that become more conductive as strain causes the gaps to shrink. This then causes a decrease in the resistivity of the bulk material. The maximum thickness of the silicone that permits quantum tunneling is called the barrier height. Different silicones can have varying barrier heights and so it is possible to find more or less conductive composites based on the silicone used. Another property of the silicone that affects the conductance is the minimum absorbed layer. This is the thinnest physical thickness that the silicone can form around a nano-particle that it is adhered to. Minimum absorbed layers have not been measured at BYU, but electrical resistance behavior changes so dramatically with different silicones that this is considered to be a contributing factor.

The previous generation of these strain gauges utilized a silicone called Sylgard 184 produced by Dow Chemical. Total volume fractions of additives ranged from 8-14% and were able to measure strains up to approximately 40%. These gauges were relatively stiff with an average Young's Modulus of 1.84MPa. Tensile failure of the material happens shortly after 40% strain [19].

Although 40% strain is an impressive range, we desired to increase the range of measured strain, while simultaneously reducing the elastic modulus of the material. This would enable an

increased range of applications with lower interference from the mechanical operation of the underlying sensor material.

Two new types of silicone were evaluated: Ecoflex and Dragon Skin, both produced by Smooth On. These silicones are much more flexible then the former Sylgard and when cured as only plain silicone, both have an elongation to break rating of over 800%. When used with nano-particle additives, strains of over 100% were still possible without compromising the integrity of the gauge. Although Dragon skin is softer and slightly more flexible, Ecoflex was found to have better properties for conductance when nano-particles were added. For this reason, Ecoflex was chosen as the silicone that would be used for future testing and experimentation.

2.4 Higher Deflections and Fewer Additives

High deflection strain gauges made from Sylgard 184 required such a high volume fraction (up to 15%) of conductive additives to attain a reasonable starting resistance that the gauges ended up being relatively stiff. Material failure also started to present at approximately 40% strain [18]. Using Ecoflex as the base material changed the composition requirements, such that combined NiNs and NCCF volume fractions only as high as 9% were needed for comparable starting resistances. The softer silicone in combination with the reduced amount of additives produced a material that was over 4 times more flexible the Sylgard gauge having a Young's Modulus of .37MPa as opposed to 1.8MPa. Figure 2.1 shows the stress/strain relationship for an Ecoflex gauge with 2% NCCF and 6% NiNs.

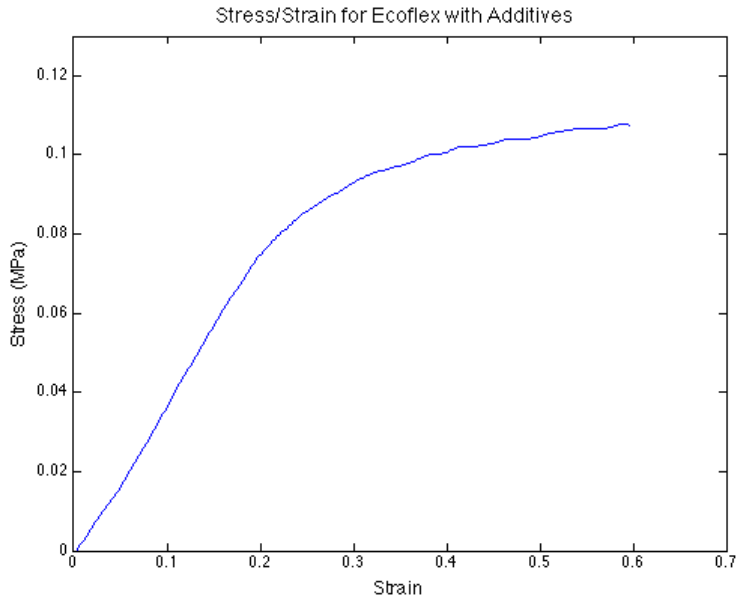

Figure 2.1 – Stress/Strain relationship for Ecoflex with 2%NCCF and 6%NiNs

With higher maximum deflections and lower stiffness, while maintaining the same level of conductivity and resistive performance, these strain gauges are more applicable for biomechanical applications then the previous generation of gauges. These sensors can be used for tracking human biometric parameters such as joint angles , chest expansion during breathing and abdominal deflections during fetal movements or labor contractions. Strain gauges made from soft silicones can be embedded into clothing or fabric, or can be applied as patches directly onto the skin without changing the mechanics of the joint or location they are fixed to. These patches or wearables could track the joint angles of a subject during activities and then by combining this data with the dimensions of known body segments, give a kinematic representation of the body. Overall, this is an excellent alternative to current motion capture methods due to its simplicity and mobility.

2.5 Gauge Manufacturing

A strict manufacturing protocol was followed throughout the entirety of this study. The main goal for gauge production was to create a material that was consistently as close to homogeneous as possible. Clumps of additives or areas with higher concentrations of NiNs and NCCF would yield inconsistent results during testing and were therefore undesirable. One of the main steps taken to avoid this problem was to fully screen all of the additives. The primary purpose of screening NiNs is to break them down to a consistent size. NiNs that have been

Figure 2.2 – NiNs being forced through a wire mesh. This process is known as "screening"

screened mix well with silicone and do not need extra attention to ensure a homogeneous mixture. On the other hand, NCCF tend to clump into small balls during storage and were screened to break up these clumps, not to further reduce the size of the fibers. Figure 2.2 depicts the setup for screening NiNs and NCCF.

The following is the process followed for manufacturing the strain gauges used in this study.

Materials Needed:

- Nickel Nanostrands
- Nickel Coated Carbon Fiber
- Novamet 526LD
- Ecoflex 2 part silicone
- SmoothOn silicone thinner
- 5ml plastic cups
- Glass stir rods
- Stirring spoons
- Thin metal spatula
- Stainless steel screen with 1mm x 1mm openings
- Laboratory scale
- Centrifugal mixer (Thinky)
- Molds
- C-clamps
- Razor blade
- Oven

Procedure:

1) Prepare NiNs and NCCF by screening. Use a spoon or glass rod to rub the materials through the metal screen until it has all been forced through.

2) While weighing on the scale, measure in the proper amounts of silicone part A, silicone part B and thinner into a 50ml cup. Remove from scale and stir by hand with glass rod. Working time of silicone is sufficient for remaining steps.
3) Put the cup back on the scale and measure in the required screened NCCF. Mix by hand with glass rod. Put cup in centrifugal mixer and mix at 2000rpm for 15 seconds. Mixture should be a shiny silver color at this point.
4) Put the cup back on the scale and measure in the required screened NiNs. Mix by hand with glass rod. Put cup in centrifugal mixer and mix at 2000rpm for 15 seconds. Mixture should be a black smooth mixture at this point with no obvious clumps of additives.
5) If clumps are present, mix by hand with glass rod again attempting to break up clumps. Put cup in centrifugal mixer and mix at 2000rpm for 15 seconds.
6) Use metal spatula to help remove all the material from the cup and transfer it into a mold.
7) Spread the material evenly throughout the mold taking care to use the spatula to push material adequately into the corners. Put the lid of the mold on and gently press it down while tapping and vibrating the lid to reduce air bubbles. Clamp the lid on lightly with a c-clamp.
8) Cure in oven at 200°c for 40 minutes.
9) Remove gauge from mold and trim off excess material with a razor blade.

2.6 Testing Procedure

In order to fully characterize the resistive behavior of the gauges with strain, a carefully controlled testing environment was required. The setup used an Instron 1321 tensile tester and a Rigol DM3068 multimeter with a maximum resistance reading capability of 110Mohm. The

specimens were clamped in electrically insolating grips with copper tabs positioned in the grips to act as electrodes for attachment to the multimeter.

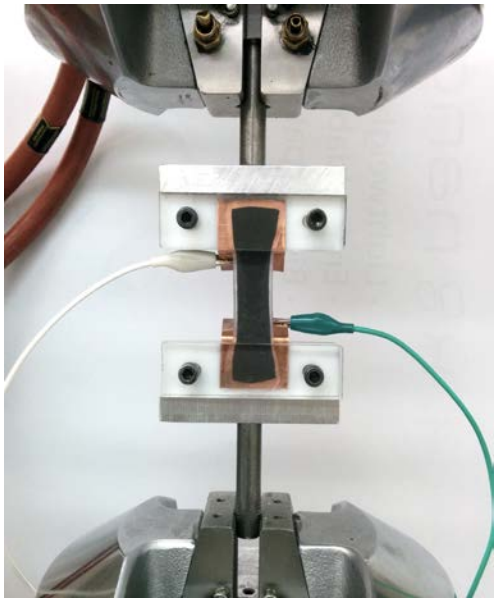

Figure 2.3 – Electrically insulated grips stretching a sample in an Instron tensile tester

Samples were stretched to a variety of strains depending on the composition and strain required to see a full change in resistance from maximum to minimum steady state. These strains ranged from 50-80%.

In the initial testing to find a suitable range of additive volume fractions to be used for a more in depth study, samples were only extended once to record their strain/resistance curves. In a more detailed design of experiments, each sample was stretched and then returned to its neutral position 5 times. The issue of permanent deformation to the gauges (discussed in the next section) required that a new neutral position be evaluated after each extension. The target strain was then evaluated based on this new neutral position.

2.7 Permanent Deformation

After a small amount of initial testing with finished gauges, it became evident that the silicone composite has a non-linear stress strain relationship that could best be described by a visco-plastic model. This means that after applying a constant load the gauge will creep or continue to elongate if the load is held and then upon unloading, there is a permanent deformation left in the material. Likewise, if a particular strain is held, the stress will decrease over time. This is a problem since changes in the material that effect the resistance while at a constant strain make using the gauge from a utility standpoint difficult since a one to one relationship for resistance and strain could not ascertained. Ecoflex by itself does not exhibit this behavior, therefore the permanent deformation was happening due to an effect of the additives. Furthermore, the problem is most obviously amplified by the proportion and length of NCCF. Although it is difficult to pinpoint the mechanical cause of this material property change, it is

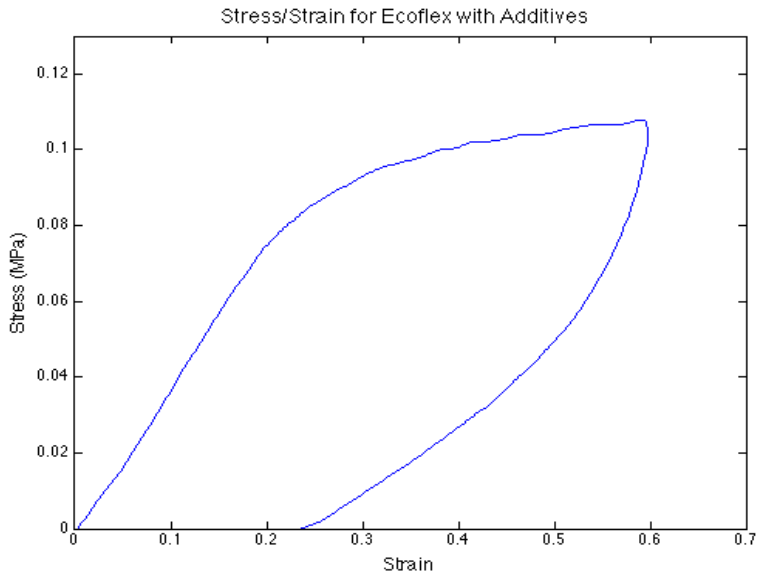

Figure 2.4 – Loading and unloading of an Ecoflex gauge with 5% NiNs and 1.5% NCCF

assumed that it has to do with interactions between the silicone and nano-particles on the inside of the gauge. As strain is applied the silicone slips over the surfaces of the additives but when released cannot completely return to its original orientation. This is more pronounced with the NCCF than the NiNs simply due to geometry. NCCF are cylindrical and smooth and more prone to the silicone slipping over their surfaces. NiNs are clumps of interwoven nickel strands and have surfaces to which the silicone can more easily bond. A gauge with only NiNs in it will still present this problem, but to a much smaller degree. Figure 2.4 displays the stress/strain relationship and the hysteresis experienced through loading and unloading. Note that with the first extension of the gauge a permanent deformation of 23% was observed.

Two measures have been taken to reduce the effects of permanent deformation in the gauges. The first is "pre-straining" or "pre-conditioning". In this method the gauge is elongated a number of times to a strain determined by its composition and susceptibility to permanent deformation. This was done in a variety of ways including stretching with grips in a tensile

Figure 2.5 – Crank roller used for pre-conditioning gauges to reduce the effects of permanent deformation.

tester, feeding through a crank roller (Figure 2.5) and stretching manually by hand. The second method was to glue the gauge onto a backing material such as a flexible fabric or elastic band.

2.8 Backings

With one of the end goals for application of the nano-composite strain gauges being integration into clothing and other wearables, finding the most effective way to apply the sensor to a backing was the natural progression for research. Not only does adhering the gauges to other materials open the door for other uses, but it also helps reduce the permanent deformation that would normally be experienced by improving the resilience of the gauge. Adding the sensor to a backing creates a system with a stiffness that can be determined by the stiffness of the material used and the type of fixation method.

A number of backing materials were tested and each provided a unique advantage over the others that could be leveraged in different applications. The 4 main materials tested were polyester fabric elastic, Kinesiology Tape, spandex and plain Ecoflex.

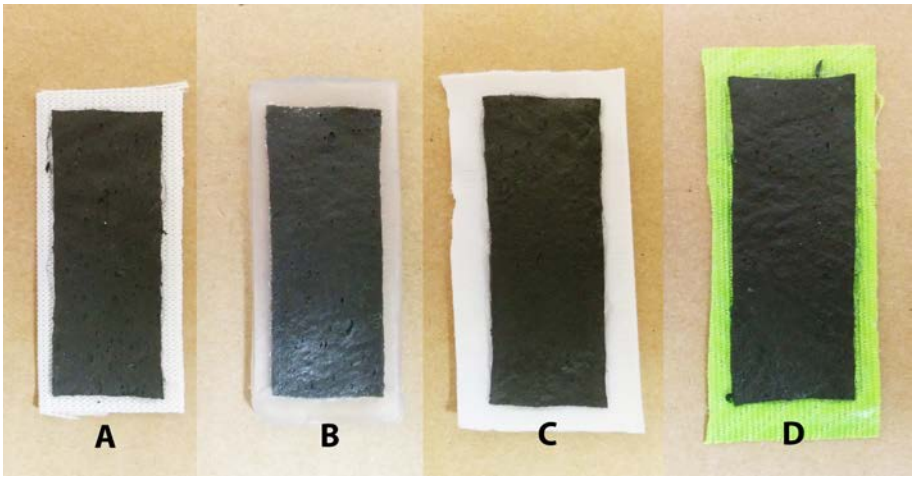

Figure 2.6 – Various backings with preconditioned gauges. A) Polyester Elastic B) Ecoflex C) Spandex D) KT Tape

Backings were tested with both preconditioned and un-preconditioned gauges glued onto them. It was found that the preconditioned sensors reached a steady state resistance curve in fewer cycles and maintained their shape better after testing was completed.

Moving forward into applications of the strain gauges, backings will be used to improve the longevity and performance of the sensors. It can also be expected that these gauges will be integrated into systems which already contain a flexible material where it would be natural to embed a sensor.

CHAPTER 3. COMPOSITION CHARACTERIZATION OF SILICONE NANO-COMPOSITE STRAIN GAUGES

3.1 Introduction

Over the last decade, there has been a proliferation of self-sensing materials that integrate mechanical function with a sensor function. Conductive composites are an example these self-sensing materials and strain detection is one of the sensing functions of which they are capable. A particular point of interest is in the area of high deflection strain sensing [20]. Despite the significant work done in measuring the response of high-deflection self-sensing materials [21] and in modeling the underlying physical phenomenon [18], to date there has been little work done in modeling the change in electrical resistance as a constitutive function of nanoparticle composition. Past research focused on a forward model that made predictions for strain/resistance relationships based on an expected response to the interactions of nanoparticles within the gauge. The model developed through this study works backwards from observed gauge behavior to determine a relationship between strain/resistance curves and volume fractions of conductive additives. This topic is highly relevant from a utility standpoint, as it enables accurate prediction of the coupled material and electrical behavior, which will allow transition out of the laboratory environment and into commercial use for applications such as adhesive strain gauge patches, sensing bushings and deformation sensing skins or membranes. Since various possible applications require different sensing properties, this study aims to model the change in electrical resistance during wide-range strain events in silicone nickel nano-composites as a function of their composition.

3.2 Background

As mechanical systems become more dynamic and as real time data analysis continues to enhance system performance, self-sensing materials are becoming more essential. The status of large deflections in a system is an example of data that can be obtained through self-sensing materials and a variety of methods have already been employed to accomplish this task. Optical sensors, fluidic strain sensors and polymers or elastomers with conductive additives are capable of measuring a wide range of strains [22]. Conducting composites can have properties allowing them to sense this type of strain and are sometimes referred to as sensing materials or smart materials. Sensing materials are used in two different contexts. In the first, the smart materials are used as sensors which augment a structure or system such as a glue-on strain gauge. In the second, structural components are made from the smart material and no auxiliary sensors are needed to report strain, damage or other vital information since the component will perform this task independently. When used in the second way, these materials are often referred to as self sensing structural materials which include but are not limited to: polymers and composites with embedded carbon fiber, concrete containing short carbon fiber strands, coatings with carbon nanotubes and many more [20, 23, 24].

When designing self-sensing composites, one of the main concerns is to meet the critical volume fraction for percolation so that the composite will be conductive [25]. Many studies have been conducted to determine the critical volume fraction and have been found to extend across a large range (0-15%), but for experimentation in this study with silicone and nickel additives, volume fractions of 6-9% have been reported as being necessary for percolation [26]. In addition, it may be noted that compositions containing additive proportions lower then the

critical volume fraction may still be useful since extreme strains themselves affect the percolation threshold by changing orientations and spacing of additives dramatically. Poisson contraction in elastomers such as those used in this study can re-orient conductive fillers to be closer to each other allowing percolation when strained even when the unstrained material is essentially nonconductive.

Nickel Nanostrands (NiNs) are made from a fine network of pure nickel, created by a chemical vapor deposition process [27]. The as-manufactured network resembles a light sponge or cake and is extremely porous. During the production process of the sensor the NiNs are forced though a screen and reduced to a filler material of fine clusters of connected nano-strands. Nickel Coated Carbon Fibers (NCCF's) are chopped at varying lengths ranging between .1mm and 1mm to provide a microscopic (as opposed to nano-scale) conductive filler that modifies the resultant conductive network in a positive manner. Using nanoparticles for embedding instead of other additives can produce enhanced physical and chemical effects due to the increased surface area to volume ratio [28]. In the case of piezo-resistive strain gauges, this increased surface area to volume ratio of the embedded particles increases the electrical capabilities of the gauge and gives a more dramatic change in the resistivity under strain.

A changing network of silicone gaps between nano and micro particles drives the mechanism for piezo-resistivity. Electrons pass through the bulk material by a means of quantum tunneling at sites where there are dislocations between filler materials. These gaps between nickel particles act are the modeled as individual resistors that produce a matrix of variable resistors, or switches [29,30] . Thus a percolation network is formed and as strain is introduced, these switches turn on and off causing the overall resistance of the material to

change. Interestingly, this material exhibits the reverse effect to that of most piezo-resistive components in that the resistance drops as it is stretched [18].

While the basic concept of high-elongation strain gauges, using the nano-composite approach outlined above, has been reported previously by the BYU research group [27, 18, 21], significant advances were required before they could be used ideally in application environments. Previous gauges were too thick and stiff to provide the sensitivity and embeddability desired. Large amounts of conductive additives were required to achieve a usable resistivity, contributing to the high stiffness of the sensors. To have an initial resistivity in the in the region of 30 kohm, material containing approximately 9% NiNs and 3% NCCF by volume was required. Earlier work produced sensors capable of tracking stretch up to 40% [18]. However, in the present work, we introduce new thinner and more flexible gauges created using a soft silicone as the base material with lower volume fractures of nanoparticles, resulting in ultra-flexible and sensitive sensors with less embedded nickel capable of achieving accurate strain tracking up to 100% stretch. To achieve the same initial resistance, proportions of NiNs and NCCF have been reduced to 5% and 1% by volume respectively

3.3 Design of Experiments

To find the relationship between additive proportions and the shape of the strain/resistance curves, an experimental design was created to gather data on unique samples with a variety of volume proportions of NiNs and NCCF. 24 samples within a known effective range of volume fractions were used to most effectively characterize the curves. This effective range was determined by a series of initial experiments within a broad spectrum of volume

fractions. Many compositions that did not exhibit a measurable resistance change were found, thereby indicating material makeups that would be avoided in the main experimentation.

In this initial experimentation, volume fractions ranging from 3-11% NiNs and .5-3% NCCF with both .5mm and 1mm being tested. Samples that contained lower then 5% NiNs and 1.5% .5mm NCCF or .5% 1mm NCCF were not conductive on a measurable scale and samples containing greater than 9% total nanoparticles (e.g., 2% NCCF and 7% NiNs) were physically poor samples due to the large amount of additives not allowing the silicone to cure properly and consistently.

It was determined that for the DOE, the volume fractions should range from 5-7% NiNs and .75-2% NCCF and that both .5mm and 1mm lengths of NCCF would be used. A 4 by 3 by 2 block design was used to provide data that would represent the entire spectrum of compositions. Table 3.1 displays the volume fractions for each sample.

Table 3.1 – Samples for DOE created. 12 unique compositions for both .5 and 1mm NCCF

	5% NiNs	6% NiNs	7% NiNs
.75% NCCF	.5mm/1mm	.5mm/1mm	.5mm/1mm
1% NCCF	.5mm/1mm	.5mm/1mm	.5mm/1mm
1.5% NCCF	.5mm/1mm	.5mm/1mm	.5mm/1mm
2% NCCF	.5mm/1mm	.5mm/1mm	.5mm/1mm

3.4 Sample Production

Material samples were manufactured using a strict method to reduce any variability that could be introduced during the production process. A silicone produced by Smooth On (EcoFlex Supersoft 0030) was used as the base material in this study. It is a 2-part silicone that requires no

catalyst and has the option of adding thinner to make the resultant material less dense and more flexible. Because raw NiNs come in larger sponge-like clusters, they were reduced to a smaller and more uniform size by rubbing them through a steel screen with .5x.5mm openings with a glass rod or spoon. For this study, sample dimensions were 100x20x1mm. Figure 3.1 describes the steps taken during manufacturing.

Manufacturing Process

1) Measuring by mass on a scale, use 1 part silicone A, 1 part silicone B and 1 part silicone thinner. (Working time is sufficient for remaining steps)
2) Weigh the required amount of NCCF then add to silicone and stir by hand.
3) Transfer to a centrifugal mixer and mix for 15 seconds at 20000rpm.
4) Remove mixture from centrifuge, weigh the required amount of NiNs then add and mix by hand. Return to the centrifugal mixer and mix for 15 seconds again.
5) Stir by hand once more and then mix in centrifuge for 15 seconds.
6) Pour/spread into mold eliminating air bubbles and clamp lightly.
7) Cure at 200°f for 40 minutes.

Figure 3.1 – Manufacturing process for sample production.

3.5 Testing

Testing of samples was done with an Instron tensile tester using custom grips designed to electrically isolate the material from the rest of the machine. Custom aluminum grips with non-conductive acrylic surface plates were used to sandwich the sample into position. Thin copper plate was glued onto the acrylic without touching the aluminum to act as a lead attachment point. Figure 4 depicts the testing setup.

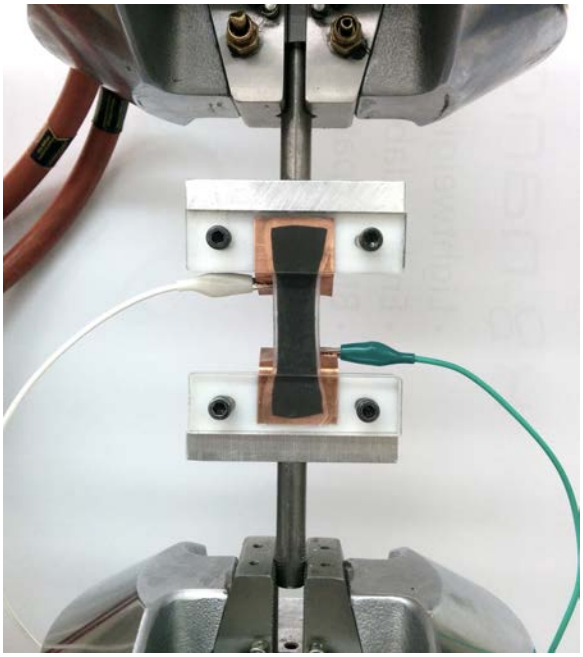

Figure 3.2 – Testing setup with insulating grips

Resistance in the sample material was measured with a Rigol 6.5 digit multimeter. Due to limitations of the device, the maximum recordable resistance was approximately 110 mega ohms. Leads ran directly from the multimeter to the copper tabs on the grips. The resistance of the leads and tabs was negligible compared to the resistance of the sample material and therefore a 4 lead sensing setup was not used.

Position and strain was determined and reported by the tensile tester and was precise to greater then 1/100 inch. Resistance and strain data was recorded and logged though a custom LabVIEW VI that matched data points from separate recording devices accurately.

Each sample underwent 5 cycles of testing to a predetermined maximum strain. It was determined from data found in the initial experimentation that the maximum strain would be different for a select number of the samples. This is because of the amount of strain required to observe the full change from maximum to minimum conductivity. Samples with high volume

fractions of NiNs and NCCF were only strained to 50% while those with lower volume fractions were taken to as high as 70% strain. Due to the visco-elastic nature of the material, each sample experienced some permanent deformation after undergoing strain and required a new neutral position to be determined after each cycle. The percent of permanent deformation decreases with each cycle, nevertheless this is a problem that will be addressed in other studies using methods of preconditioning and applying backing materials to the gauges.

Results from testing the 24 samples found that it was appropriate to divide the sample into 2 categories: low resistance and high resistance. Low resistance samples were conductive on a measurable scale at 0 strain and remained measurable through their whole extension. High resistance samples were either not initially conductive or had the resistance go above the measuring capabilities of the multimeter during straining. Figures 3.3 and 3.4 show the 5th cycle of each sample that produced viable data.

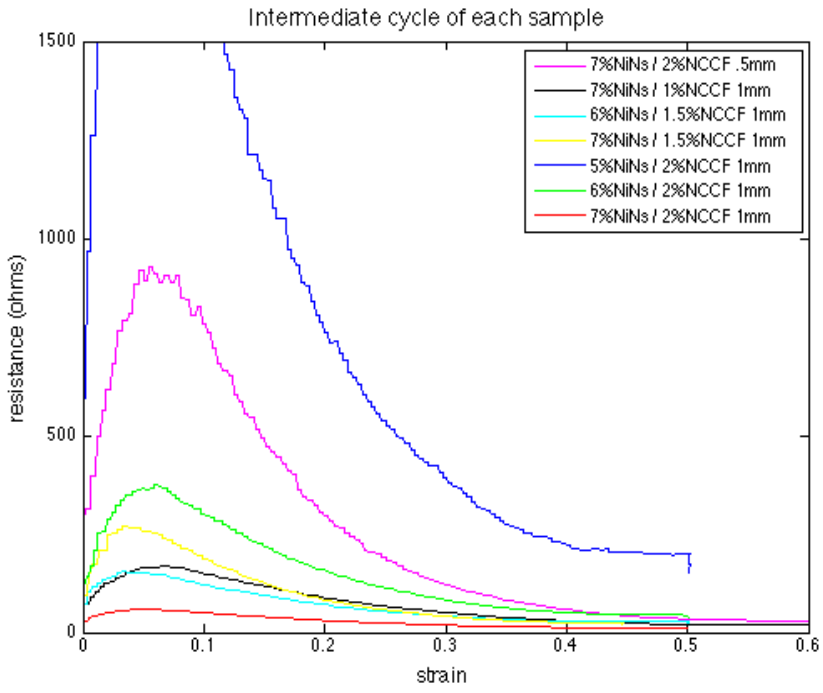

Figure 3.3 – Strain/resistance curves for samples considered to be “low resistance”

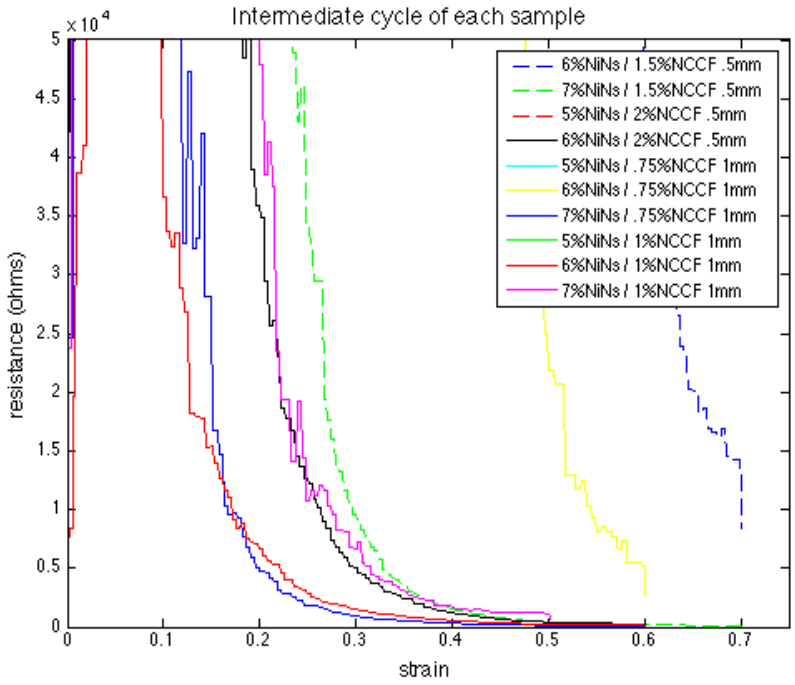

Figure 3.4 – Strain/resistance curves for samples considered to be "high resistance"

It is also important to note that some compositions never became conductive within the measuring capabilities. From the data found during the initial experimentation, it was assumed that some of the compositions listed in Figure 1 would not provide useable results, but were made and tested regardless. For example, the .75% NCCF with 5% NiNs was found to give useful data with 1mm length NCCF but not with .5mm fibers.

3.6 Modeling

Based on the shape of the raw resistance/strain data set, a modified log-normal distribution was used to model the response. The unaltered log-normal distribution (Eq. 1) has a shape parameter A and a location parameter B. The modified log-normal equation (Eq. 2) adds in a x-axis scaling parameter C and a y-axis scaling parameter D but eliminates the position parameter B.

$$\frac{1}{ax\sqrt{2\pi}}\exp\left(-\frac{(\ln(x-b))^2}{2a^2}\right) \quad \text{(Eq.1)}$$

$$d\cdot\left[\frac{1}{a\left(\frac{x}{c}\right)\sqrt{2\pi}}\exp\left(-\frac{ln\left(\frac{x}{c}\right)^2}{2a^2}\right)\right] \quad \text{(Eq.2)}$$

Table 3.2 – Parameters and R^2 values for curve fit models of all samples.

1mm NCCF / .5mm NCCF	5% NiNs	6% NiNs	7% NiNs
.75% NCCF	Not Conductive	A = .28 C = .095 D = 1.2e11 R^2 = .897	A = .59 C = .043 D = 7.39e5 R^2 = .914
	Not Conductive	Not Conductive	Not Conductive
1% NCCF	Not Conductive	A = .53 C = .065 D = 1.32e5 R^2 = .966	A = 1.1 C = .19 D = 248.9 R^2 = .993
	Not Conductive	Not Conductive	Not Conductive
1.5% NCCF	A = .61 C = .021 D = 8.85e6 R^2 = .791	A = 1.19 C = .185 D = 226.6 R^2 = .984	A = 1.1 C = .125 D = 406.6 R^2 = .997
	Not Conductive	A = .38 C = .11 D = 1.0e10 R^2 = .743	A = .47 C = .075 D = 9.09e6 R^2 = .703
2% NCCF	A = 1.0 C = .125 D = 3472.2 R^2 = .982	A = 1.05 C = .148 D = 573.6 R^2 = .981	A = 1.4 C = .28 D = 76.9 R^2 = .987
	Not Conductive	A = .66 C = .066 D = 1.155e6 R^2 = .926	A = .82 C = ..113 D = 1363 R^2 = .993

Equation 2 was used to find best fit curves to the raw strain/resistance data so that the parameters A, C and D could be found for each gauge composition. Good fits were found with an average R^2 value of .93. Table 3.2 reports the parameters for these curve fits.

The most noticeable trends are the reduction of D as you move from the top left to the bottom right of the chart and the increase in A in the same fashion. These trends motivated a statistical analysis of the parameters to find correlation with the percentages for volume fractions.

A standard least squares regression analysis performed with the statistical software JMP evaluated the relationship between curve fit parameters and volume fractions. This linear regression t-test with NiNs and NCCF as the dependent variables yielded p-values significant at the .05 level. Analysis was only done for samples containing 1mm NCCF because of how few samples containing .5mm NCCF were conductive.

Prediction equations for relationships between parameters were found and are given in terms of volume fractions of NiNs and NCCF. These equations are given in table 3.3. The p-values for the significance of these fit prediction values are shown in table 3.4.

Table 3.3 – Prediction equations for fit parameters

A	-1.3481 + .5494*NCCF + .2397*NiNs
Logit(C)	-8.8278 + 1.3504*NCCF + .7576*NiNs
Log(D)	39.6426 – 6.3161*NCCF – 3.500*NiNs

Table 3.4 – p-values for significance between curve fit parameters and volume fractions

	NiNs	**NCCF**
A	.026	.009
Logit(C)	.047	.044
Log(D)	.040	.036

Table 3.5 – Curve fit parameters based on prediction model.

1mm NCCF	5% NiNs	6% NiNs	7% NiNs
.75% NCCF	Not Conductive	A = .50 C = .037 D = 1.094e6	A = .74 C = .075 D = 3.304e4
1% NCCF	Not Conductive	A = .64 C = .0506 D = 2.256e5 R^2 = .66	A = .88 C = .102 D = 6.812e3
1.5% NCCF	A = .67 C = .047 D = 3.176e5	A = .91 C = .095 D = 9.59e3	A = 1.15 C = .183 D = 289.6 R^2 = .77
2% NCCF	A = .95 C = .088 D = 1.35e4	A = 1.19 C = .17 D = 407.6 R^2 = .73	A = 1.42 C = .305 D = 12.3

Using the prediction equations, the three curve fit parameters can be described in terms of %NiNs and %NCCF. By substituting these equations into Equation 2, a model for a predicted strain/resistance curve is given with only 2 parameters instead of 3. Table 3.5 shows the parameters estimated using this method.

For some compositions, the model was effective at predicting the strain/resistance curve. The model has difficulty predicting D most likely due to the magnitude of its exponential growth moving from the bottom right to top left of the table. Figure 3.5 depicts the final comparison between the raw data, a 3-parameter curve fit and the prediction model.

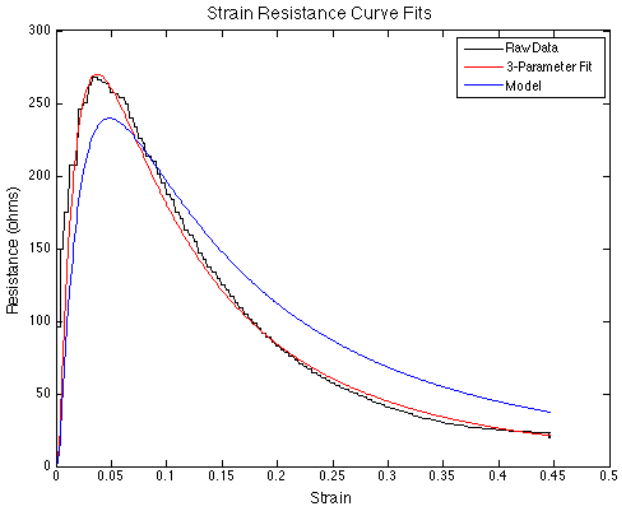

Figure 3.5 – Comparison between acquired data, a modified log-normal 3 parameter curve fit and the model based on the prediction equations for A,C and D.

3.7 Discussion

For this study, threshold volume fractions of additives for percolation were pre-determined and the model is meant to describe what happens around that volume fraction. Some samples were not conductive until a certain degree of strain was applied and others experienced such drastic changes that we can assume that strain also influences percolative behavior by the

change in spacing and orientation amongst nanoparticles. A composite that does not have a high enough volume fraction of conductive additives to initially form a percolative network may become so under strain since more junctions become conductive resulting in a percolative network.

When dealing with conductive additives in an elastomer, the spacing between particles has been described by a probability distribution [2,18]. The shape of this distribution changes with strain and the number of conducting gaps between particles can increase, therefore reducing the bulk resistivity of the material. Figure 3.6 depicts a hypothetical example of these distributions changing with strain. Note that although the density of large gaps increases the same and the density of small gaps, the small gaps experience a greater increase in conductivity

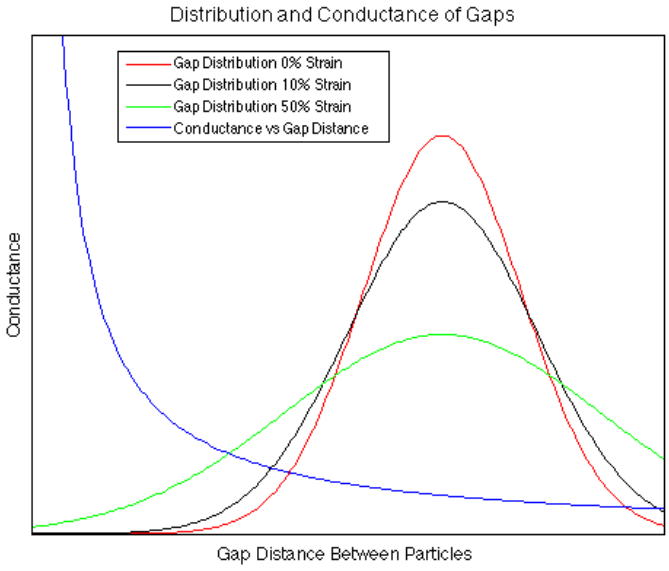

Figure 3.6 – Gap distances with strain and gap conductance

then the decrease experienced by the large gaps. This is an abbreviated explanation of how gap distributions change, but a more detailed explanation can be found in other literature [2]. By examining the data (Figures 3.3 and 3.4), it is observed that most of the samples (primarily those

in the low resistance group) experience an initial increase in resistance followed by a decrease. The high resistance samples do not all exhibit this behavior, but this may be due to the limitations of the measurements. It is presumed that the increase in resistance is cause by the differences in the proportions of large and small gaps. In the first 10% strain, the gaps that become larger overpower the gaps that become smaller since the smaller gap's do not experience any great increase in conductivity. It is not until the material is deformed to a higher strain that the small gaps conductivity drastically increases and overpowers the number of large gaps thereby lowering the bulk resistivity. The shape of the curves can now be discussed in terms of the values found for the curve fit. The value of the A parameter effects the general shape the curve. Lower A values produce a shape that is more like a normal distribution curve while higher values for A skew the curve to the right and move the peak to the left. The general trend observed in the results for A is that it increases from lower volume fractions to higher volume fractions of additives. This indicates that samples with more additives undergo a quicker transition to peak resistance at a lower strain and then a more gradual transition to its minimum resistance at a higher strain. A may be a descriptor of how rapidly the gap distributions change with strain. The value of the D parameter is most closely associated with the scale of the peak resistance. It increases and decreases with respect to the amount of conductive additives in the material. This is most likely related to a shift in the mean gap distance where the average gap is smaller when D is lower. C does not show any easily recognizable trend in the data and is therefore difficult to determine what it represents in terms of the resistive behavior of the material.

The regression analysis done for this study indicated that for the 3-parameter version of the curve fit the variables A, C and D were strongly related to the NiNs and NCCF concentrations. This agrees with the trends visible in the data seen in tables 3.2 and 3.3.

This analysis is lacking in power due to the sample size and could be improved to find more meaningful results by increasing the sample size and number of duplicates within each sample type.

3.8 Conclusion

This study was able to model the resistance versus strain curves for a wide variety of compositions of nickel nano-composite strain gauges. The model is based on a log-normal distribution which provided good fits with the data at an average R^2 value of .92. A strong statistical correlation was found between curve fit parameters and additive volume fractions indicating that the modified lognormal fit functions well for this model.

The variety of curve shapes for different compositions during testing (figures 4 and 5) great potential for a number of applications. Resistance behavior of the material has the capability of being customized to the needs of the situation to where it is to be applied. For example a composition with fewer additives like many of the high resistance samples could be used as strain threshold detectors since they "switch" from insolating to conductive in such a small amount of strain. On the other hand a composition containing more additives could be used as a continuous strain sensor for strains up to approximately 50%.

Currently, the log-normal curve fit model would allow for a shape to be picked in terms of the parameters of the equation, and then a composition determined through solution to the system of equations found in table 3.3. This method can be verifired by following the process

above and then comparing results between the modeled curve and actual data. This is a useable method for finding desired compositions but can be improved upon when more definitive relationships are found between curve fit parameters and volume fractions of additives through a more robust statistical analysis.

CHAPTER 4. FETAL MONITORING AND OTHER APPLICATIONS

4.1 Introduction

The new gauges developed through this research are capable of stretching to 100% of their original length or greater while having a sensing bandwidth sufficient to detect small movements. This has opened the door to a variety of applications. The sensor consistency and feel is similar to that of skin making it natural to apply these sensors in the area of biomechanics. Currently, an examination of a variety of techniques for fastening the sensors to humans is being conducted including the use of patches, integrated tapes, paint on methods and others. Eventual applications include joint tracking, as well as muscle and skin movement during physical activity. This study has focused on maternal biometrics during pregnancy.

Figure 4.1 – Fetal monitoring device prototype

Fetal monitoring is an area of the medical field where only a few methods exist for detecting fetal movements and labor contractions. None of them are simple or mobile and all require doctor or nurse supervision in hospitals or other birthing locations. Since labor contractions and fetal movements such as kicks can be large enough to be visually noticeable on the outside of the abdomen, a prototype for a deflection driven monitoring system has been developed leveraging the strain sensing capabilities of the nano-composite gauges. Changes in dimension to the abdomen of a pregnant woman can be tracked and reported wirelessly to a computer or smart phone to log events of interest. This study will describe the work to date on the development and testing of the fetal monitoring device.

4.2 Background

The best indicator for labor progress is currently the timing of contractions including duration and intervals in between them. However, fetal and contraction monitoring systems are not universally used in the hospital to assist doctors during child deliveries and are rarely used to monitor the increasing number of home births. One reason for this is that existing monitoring systems are obtrusive, uncomfortable, and tether the expectant mother to bulky monitoring hardware.

Three main methods exist for measuring the duration and frequency of uterine contractions during labor [31, 32]. Tocodynamometry and electrohysterography (EHG) are external measurement methods while intra-uterine pressure catheters (IUPC's) are an internal option. Tocodynamometry utilizes displacement tracking of a plunger depressed by the outward force of the contracting uterus [33]. It succeeds at providing contraction frequency and approximate duration, but fails in that it requires frequent nurse attention to keep in place and

often will not even work on obese patients whose external manifestations are masked. In a study of 50 obese and 50 normal women by Ray et al [34], 26% of morbidly obese women required internal monitoring while 0% of women with normal BMI required it. These complications and others such as body movement or muscle action occur frequently enough to require the other monitoring methods such as IUPC's or EHG's.

IUPC's are the most accurate for identifying contractions [35]. Not only do they detect contraction frequency and duration, but they also detect the uterine pressure giving data on the intensity of the contraction while ignoring uterine changes due to other movements of the body. As effective as this method is, it is avoided due to the potential for infection since tissue must be ruptured (water must be broken) for an IUPC to be inserted. It also requires more time and attention from the doctor as compared with other devices that can be handled by the nurses or staff.

Electrohysterography uses electrodes to detect the electrical activation during contractions in the uterus [36, 37, 38, 39]. One study has shown that agreement between IUPC and EHG methods can range between 60% and 75% depending on the threshold level for contraction criterion [40, 41]. An electrohysterogram is superior to the tocometer in that it is not affected by maternal movements. EHG's are also being looked into as a way to detect preterm labor which is one of the leading causes of fetal mortality [42]. The down side to EHG is that it requires a substantial number of electrodes and leads in order to obtain accurate results. The increased number of leads encumber the expectant mother, causing immobility and discomfort.

The downfalls of the current methods for fetal monitoring are the motivation behind the development of the deflection driven device. By using the changing size of the abdomen as the indicator for fetal activity, the complexity of the device can be reduced by using a single strain

gauge as the sensor. Its mobility, user friendliness and cost are clear advantages over current technology.

4.3 Sensor Selection

Since the nano-composite strain gauge is the pivotal component of the fetal monitoring device, a great deal of effort was dedicated to finding the ideal composition. Based on an evaluation of over 24 unique material compositions, the final sensor chosen for use in this study was composed of Eco Flex silicone with 6% NiNs and 2% NCCF by volume. This composition had the largest sensing bandwidth and a curve with a relatively linear region that would work well for correlating resistance to strain. The gauge was manufactured using the same method previously described in this work and was cured in a 100mm x 20mm x 1mm mold. The sensor was then cut to final dimensions planned for the device. Initially, copper mesh electrodes were embedded into extreme ends of the sensor prior to curing to provide a robust electrical attachment to the sensor. With extended use these electrodes proved to tear out and damage the sensor therefore requiring a different method for electrical attachment. Flexible silver infused fabric was found to be a suitable replacement [43]. It could be glued to the surface at the ends of the sensor and even span the flexible area of the system where a rigid wire would need configuring to account for the sensor extension.

4.4 Microcontroller Platform

During testing of the HDSG's, a precise ohmmeter was used to directly read resistance. As development of the fetal monitoring device moved into prototype preparation, a compact microcontroller was used to read voltage drop across the gauge instead of direct resistance. The

RFD22301 microcontroller produced by RFduino was selected for its size, power consumption, number of available analog channels and Bluetooth capabilities. It requires a 3.3V power supply.

A Wheatstone bridge voltage divider was used to amplify the voltage drop so that the microcontroller could more easily detect the change (Figure 14). In a typical Wheatstone bridge the resistor in series with the strain gauge should have a close to matching resistance. Due to the large changes in resistance that happen with these nano-composite gauges, it is difficult to select the proper resistance for the resistor in series. It was found that using a 1Mohm worked for most gauge compositions and is recommended as a good intermediate resistance.

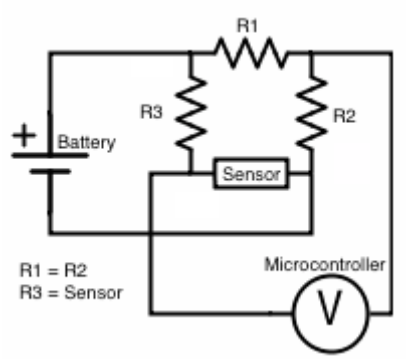

Figure 4.2 – Wheatstone bridge schematic

The RFduino microcontroller acts as the voltmeter in this Wheatstone bridge. The sensing wire is connected to an analog pin where the output it represented at a number between 0 and 1023 which represents a scaled voltage. With calibration based on know strains and corresponding resistances, these values are set to give a strain reading.

4.5 Prototype Development

The initial prototype was designed as an adjustable belt that could be fastened around the abdomen a pregnant woman. It was constructed of a non flexible webbing with a small section

of flexible fabric in the front where the sensor is placed. This was done so that all of the circumferential strain in the abdomen that occurs during a fetal movement or contraction will be expressed in the sensor.

Typical abdominal size changes seen during contractions are approximately 1cm over the circumference. With the selected gauge composition (2%NCCF 6%NiNs) having an effective strain sensing capability up to 40%, the ideal length of the sensor would be 5cm. This gives a total possible change in circumference of 2cm, which is sufficient to provide good resolution in the results, but also account for larger then average abdominal deflections.

Currently, a unique calibration is needed for each sensor produced. This is because of the extreme sensitivity of the strain/resistance relationship to composition and the inability to perfectly manufacture gauges. With larger scale development, many sensors could be manufactured from one batch with a common calibration for all of them.

4.6 Simulation Testing

A contraction simulator was conceived to mimic the dimensional changes of the abdomen during labor contractions to show proof of concept and to ensure that the sensing capabilities of the strain gauge were adequate for this application. A utility ball was placed in a depressing mechanism that could be actuated using lever to cause the ball to be compressed and expand uniformly around its circumference.

Figure 4.3 – Contraction simulator. A utility ball is depressed and released to simulate the circumferential change of the abdomen.

For the average woman, a contraction can cause a dimension change of approximately 1cm-2cm around the abdomen. Data and reports on the dimensional changes of the abdomen during contractions are sparse. Abdomen circumference is not a body statistic that medical researcher are concerned with and have not published this information. The values used in this study are based on informal literature and anecdotal responses from local obstetricians. A flexible tape measure was used to quantify the circumference of the utility ball for calibration with the sensor signal. Contractions were simulated with varying durations and intervals in between. Although normal contractions can last as long as 2 minutes and be as long as 20 minutes apart, for convenience during testing, the durations and intervals were limited to one minute each. Note that during this testing, the Bluetooth wireless microcontroller as not used. A

wired Arduino was used instead. Figure 4.4 shows the raw analog data as recorded by the controller.

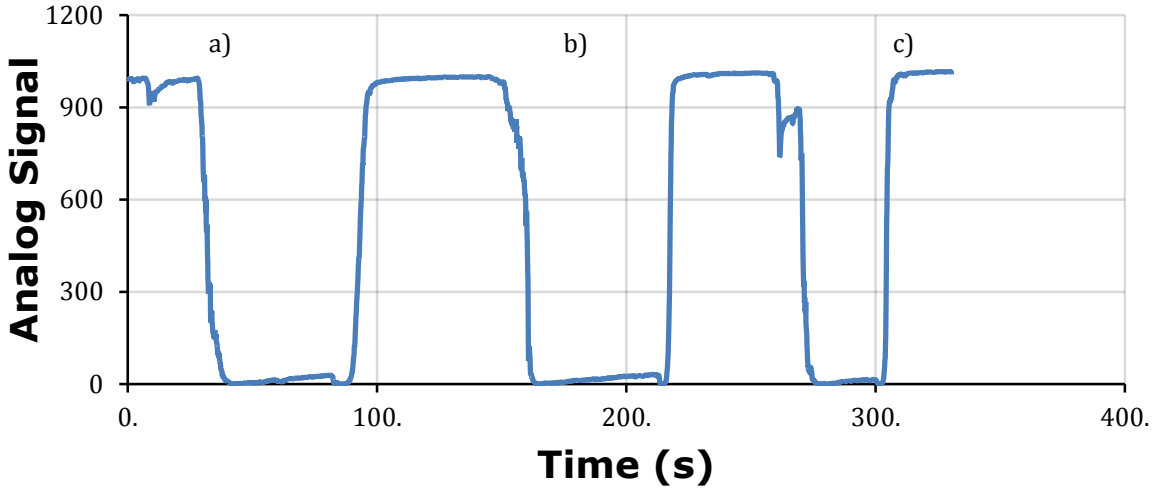

Figure 4.4 – Analog signal as contractions are simulated by fluctuating the circumference of the utility ball. a) 1 minute contraction initiated b) 1 minute contraction c) 30 second contraction

4.7 Discussion and Future Work

The differentiation between simulated contractions and uterine inactivity is clear. The nano-composite strain gauge is capable of detecting dimensional changes of a shape that is similar to the pregnant abdomen. With proper calibration this device proves itself as a feasible option for fetal monitoring in term of tracking contractions.

A small amount of initial testing for noise due to maternal movements was done. The subject was observed wearing the belt while performing regular activities such sitting, standing, walking, laying down and bending over. Some movements such as going from standing to sitting caused a disturbance to the fetal monitoring device that would require recalibration or a signal that appeared to be sustained activity. Movements of the belt due to walking or breathing

did not produce an excessive amount of noise that would interfere with the monitoring. Most sources of noise could be recognized through programming thresholds into the software that ignored fluctuations other then those known to match the frequency and duration of fetal movements and contractions. More testing would be required to fully determine the effects of maternal movements on signal clarity from the sensor.

The most important indicators for labor progress from contraction monitoring are the frequency and duration of the contractions. Intensity of the contractions has not been found to be significantly related to any component of labor progress. With this in mind, the most important duty of a fetal monitoring device is to accurately log the events which indicate the beginning and end of a contraction.

The simplicity of monitoring with the strain gauge device as opposed to the tocodynamometer is an obvious advantage. This device could be used at home or in many situations where the equipment necessary for monitoring with a tocodynamometer or other device is not available. The tocodynamometer is also an expensive device which limits it's use to locations that can afford to have one. One of the main disadvantages of the tocodynamometer is that it needs careful placement to ensure a good reading and is easily moved by maternal movements. The strain gauge fetal monitoring belt is lower profile and can be fastened onto the mother more securely, especially with the plans to incorporate the device into existing maternity accessories. The tocodynamometer could easily be adapted to use a different fastening method to alleviate this concern.

The fetal monitoring belt is intended to function as a proof of concept device. The endpoint goal is to have the sensor integrated into clothing or an accessory that pregnant woman already use. One such accessory is the Bella Band which is a flexible tube that mothers wear

over their belly and upper pants so that buttoning her pants is unnecessary. Multiple sensors could be placed on this accessory over the abdomen to gain a better mapping of the deformation during fetal movements.

4.8 Conclusions

For the contraction monitoring belt, we found that the sensing ability of the system is very promising. The contraction monitor is highly sensitive to circumferential changes in the abdomen. With such drastic changes in electrical resistance through only 8mm of circumference change we expect that the belt is sensitive enough to detect actual shape changes to the abdomen due to contractions during labor. By incorporating a microcontroller and wireless Bluetooth transmission module, we anticipate that integration of the sensor with a smartphone or tablet will provide significant advantages in terms of cost, comfort, and mobility over existing technologies for monitoring contractions during labor.

CHAPTER 5. OVERALL CONCLUSIONS AND FUTURE WORK

This research has succeeded in improving the usability of the silicone nickel nano-composite strain gauges. These strain gauges are closer to the stiffness of skin, making them more appropriate for tracking biometrics. Solutions to the issue of permanent deformation were presented including methods for applying backings and preconditioning the sensors. Ongoing work includes a of study fixation methods for attaching the sensor to the backings. Methods such as sewing, gluing and molding directly onto substrates are being explored.

Through the block experiment designed to characterize the strain/resistance curves for various compositional makeups of the strain gauges, an excellent curve fit and model were created to describe the behavior of the nano-composite material. An equation based on the log-normal distribution was used to match a curve to the data plots found with an average R^2 value for goodness of fit being .93. The model was validated by a standard least squares statistical analysis which found prediction equations for the relationship between fit parameters and volume fractions with good significance at the .05 level.

The high quality of the fit may be an indication of some physical phenomenon that is taking place in the strain gauges. Future work could include a deeper study of the shape of these strain/resistance curves to determine if the original multi-scale model for the physics of this material can be altered. This may be something that can be done regardless, taking into account the different material properties of the new silicone.

This research has also shown the feasibility of a deflection driven fetal monitoring device for tracking labor contractions and other fetal movements such as kicks. Simulations have shown that the system is capable of detecting deflections on a spherical surface similar to the magnitude of that which would be evident with labor contractions.

The direction for work on this device is to take it from a lab setting and prepare it for the end user. This will involve a shift from the belt-oriented design toward a prototype that is integrated into existing clothing or accessories that pregnant women are already using. Also included in ongoing and future work is the development of the software for tracking contractions and fetal movements. An application for Apple or Android will allow users to view data on the status of their fetal movements in real time and automatically log important events.

Although not related to the study of the strain gauge technology, a heart rate monitoring system is also an equally important part of fetal monitoring. Miniature Doppler devices currently exist that could easily be adapted for use as the heart rate monitor for this system.

The future for the use of silicon nickel nano-composite strain gauges in application settings is broad and promising. A myriad of ideas and concepts have been discussed and currently a wristband and/or finger device is being prototyped for use as a computer interfacing tool. Movement of the wrist or fingers would be tracked by strain gauges placed across the joints of interest so that haptic feedback could be used to send commands to the computer or device. This is only the beginning of what can be done with the versatile nano-composite strain gauge!

REFERENCES

1. Window, A.L., "Strain gauge technology". 2nd ed. 1992, London ; New York: *Elsevier Applied Science*. xii, 358 p.

2. Haslach, H.W., Jr. and J.S. Sirkis, "Surface-mounted optical fiber strain sensor design". *Appl Opt*, 1991. **30**(28): p. 4069-80.

3. Marvin, D.C. and N.A. Ives, "Wide-range fiber-optic strain sensor". *Appl Opt*, 1984. **23**(23): p. 4212-7.

4. Kiesel, S., "Behaviour of intrinsic polymer optical fibre sensor for large-strain applications". *Measurement Science and Technology*, 2007. Volume 18 (10).

5. Kleckers, T., "Optical versus electrical strain gages: A comparison". *HBM Measurements* 2007.

6. Cheng, C.C., et al., "Estimations of fiber Bragg grating parameters and strain gauge factor using optical spectrum and strain distribution information". *Appl Opt*, 2007. 46(21): p. 4555-62.

7. Celander, O. and G. Thunell, "The mercury-in-rubber strain gauge for measurements of blood pressure and peripheral circulation in newborn infants". *Acta Paediatr*, 1961. 50: p. 505-10.

8. Raman, E.R., et al., "Venous occlusion plethysmography with mercury-in-rubber strain gauges". *Acta Anaesthesiol Belg*, 1980. 31(1): p. 5-14.

9. Park, J., et al., "Material Approaches to Stretchable Strain Sensors". *Chemphyschem*, 2015.

10. Qiu, W., et al., "Strain sensor of carbon nanotubes in microscale: from model to metrology". *Scientific World Journal*, 2014.

11. Knite, M., et al., "Elastomer-carbon nanotube composites as prospective multifunctional sensing materials". *J Nanosci Nanotechnol*, 2009. 9(6): p. 3587-92.

12. Cohen, D.J., et al., "A highly elastic, capacitive strain gauge based on percolating nanotube networks". *Nano Lett*, 2012. 12(4): p. 1821-5.

13. Nanshu, C.N., "Highly Sensitive Skin-Mountable Strain Gauges Based Entirely on Elastomers". *Adv. Funct. Mater*, 2012.

14. Tjahyono, A.P., "A novel polypyrrole and natural rubber based flexible large strain sensor". *Sensors and Actuators B: Chemical*, 2012. 166–167: p. 426–437.

15. Boland, C.S.e.a., "Sensitive, High-Strain, High-Rate Bodily Motion Sensors Based on Graphene–Rubber Composites". *ASC Nano*, 2014. 8(9).

16. Li, X., et al., "Stretchable and highly sensitive graphene-on-polymer strain sensors". *Sci Rep*, 2012. **2**: p. 870.

17. Kyrylyuk, A.V., et al., "Controlling electrical percolation in multicomponent carbon nanotube dispersions". *Nat Nanotechnol*, 2011. 6(6): p. 364-9.

18. Johnson, O.K., et al., "Optimization of nickel nanocomposite for large strain sensing applications, in Sensors & Actuators". *A. Physical*. 2011. p. 40-47.

19. Remmington, T.D., "Biomechanical Applications and Modeling of Quantum Nano-Composite Strain Gauges". *BYU ScholarsArchive*, 2014.

20. Tadakaluru, S., W. Thongsuwan, and P. Singjai, "Stretchable and flexible high-strain sensors made using carbon nanotubes and graphite films on natural rubber". *Sensors (Basel)*, 2014. 14(1): p. 868-76.

21. Hyatt, T., "Piezoresistive nano-composites : characterization and applications". 2010, *Brigham Young University. Dept. of Mechanical Engineering*, 2010.

22. Cheung, Y.-N., et al., "A novel fluidic strain sensor for large strain measurement, in Sensors & Actuators". *A. Physical*. 2008. p. 401-408.

23. Chung, D.D., "Self-monitoring structural materials". *Materials Science and Engineering: R: Reports*, 1998. 22(2): p. 57-78.

24. Allred, D.D., et al., "Strain-based Electrical Properties of Systems of Carbon Nanotubes Embedded in Parylene". *Materials Research Society*, 2007

25. Kyriaki, K., F. Hiroyuki, and T.D. Lawrence, "A Route for Polymer Nanocomposites with Engineered Electrical Conductivity and Percolation Threshold". *Materials*, 2010. p. 1089.

26. Mandal, B., "Conducting polymer nanocomposites with extremely low percolation threshold". *Bulletin of Materials Science*. 1998. p. 161-165.

27. Koecher, M., "Characterization of Nickel Nanostrand Nanocomposites through Dielectric Spectroscopy and Nanoindentation". *Polymer Eng & Sci*, 2011.

28. Deepshikha, T. and T. Basu, "A Review on Synthesis and Characterization of Nanostructured Conducting Polymers (NSCP) and Application in Biosensors". *Analytical Letters*. 2011, Taylor & Francis Group. p. 1126-1171.

29. Karimi, F., M. Fathipour, and R. Hosseini, "A quantum mechanical transport approach to simulation of quadruple gate silicon nanowire transistor". *J Nanosci Nanotechnol*, 2011. 11(12): p. 10476-9.

30. Zeng, X.M., et al., "Characteristics of the Electrical Percolation in Carbon Nanotubes/Polymer Nanocomposites". *Journal of Physical Chemistry C*. 2011. p. 21685-21690.

31. Euliano, T.Y., et al., "Monitoring uterine activity during labor: a comparison of 3 methods". *Am J Obstet Gynecol*, 2013. 208(1): p. 66 e1-6.

32. Hadar, E., et al., "A comparison between electrical uterine monitor, tocodynamometer and intra uterine pressure catheter for uterine activity in labor". *J Matern Fetal Neonatal Med*, 2014: p. 1-8.

33. Freeman, R.K., G. Anderson, and W. Dorchester, "A prospective multi-institutional study of antepartum fetal heart rate monitoring. II. Contraction stress test versus nonstress test for primary surveillance". *Am J Obstet Gynecol*, 1982. 143(7): p. 778-81.

34. Ray, A., A. Hildreth, and U.I. Esen, "Morbid obesity and intra-partum care". *J Obstet Gynaecol*, 2008. 28(3): p. 301-4.

35. Bakker, J.J., et al., "Internal versus external tocodynamometry during induced or augmented labour". *Cochrane Database Syst Rev*, 2013. 8: p. CD006947.

36. Jezewski, J., et al., "Quantitative analysis of contraction patterns in electrical activity signal of pregnant uterus as an alternative to mechanical approach". *Physiol Meas*, 2005. 26(5): p. 753-67.

37. Maul, H., et al., "Non-invasive transabdominal uterine electromyography correlates with the strength of intrauterine pressure and is predictive of labor and delivery". *J Matern Fetal Neonatal Med*, 2004. **15**(5): p. 297-301.

38. Jacod, B.C., et al., "A validation of electrohysterography for uterine activity monitoring during labour". *J Matern Fetal Neonatal Med*, 2010. 23(1): p. 17-22.

39. Steer, P.J., "Standards in fetal monitoring--practical requirements for uterine activity measurement and recording". *Br J Obstet Gynaecol*, 1993. 100 Suppl 9: p. 32-6.

40. Haran, G., et al., "A comparison of surface acquired uterine electromyography and intrauterine pressure catheter to assess uterine activity". *Am J Obstet Gynecol*, 2012. 206(5): p. 412 e1-5.

41. Euliano, T., et al., "Prediction of intrauterine pressure waveform from transabdominal electrohysterography". *J Matern Fetal Neonatal Med*, 2006. 19(12): p. 811-6.

42. Marque, C.K., et al., "Preterm labour detection by use of a biophysical marker: the uterine electrical activity". *BMC Pregnancy Childbirth*, 2007. 7 Suppl 1: p. S5.

43. Park, M., et al., "Highly stretchable electric circuits from a composite material of silver nanoparticles and elastomeric fibres". *Nat Nanotechnol*, 2012. 7(12): p. 803-9.